Mechanisms of Electrophilic Substitutions of Aliphatic Hydrocarbons: $CH_4 + NO^+$

Peter R. Schreiner,[1a,b] Paul von Ragué Schleyer,*[,1a,b] and Henry F. Schaefer, III*[,1a]

Contribution from the Center for Computational Quantum Chemistry, The University of Georgia, Athens, Georgia 30602, and Institut für Organische Chemie der Universität Erlangen-Nürnberg, Henkestrasse 42, D-91054 Erlangen, Germany

Received May 5, 1993®

Abstract: The substitution reaction of methane with the nitrosonium cation, a model electrophile, was investigated computationally at the Hartree–Fock and correlated MP2, MP4SDTQ, and CISD levels of theory, using standard basis sets (6–31G(d), 6–31G(dp), and 6–31+G(dp) for geometry optimizations and TZ2P for energy single points on the most critical structures). The energetically favored reaction course leads to N-protonated nitrosomethane, H_3CHNO^+ (**6**). The initial complex of CH_4 and NO^+ in C_s symmetry is bound by –3.7 kcal mol^{-1} (MP4SDTQ/6–31+G(dp)//MP2/6–31+G(dp) + ZPVE//MP2/6–31+G(dp)). In the critical step, the electrophile NO^+ attacks carbon directly, rather than a C–H bond, to yield a pentacoordinate intermediate (**3**) with a hydrogen unit attached to a H_2CNO^+ cation moiety [ΔH_0(CISD+Q/TZ2P//MP2/6–31G(dp)+ZPVE//MP2/6–31G(dp)) = 57.3 kcal mol^{-1}]. This unusual mode of attack, proceeding through a transition structure which also has three-center two-electron (3c–2e) CHH bonding, can be visualized in two ways. During the reaction, tetrahedral methane distorts to lower symmetry (C_s) and binding between the electrophile and the developing lone pair occurs. The energy required for the methane distortion is partly recovered from the new bonding interaction to the electrophile. An alternative pathway involving the insertion of NO^+ into a CH bond is less favorable by 14.4 kcal mol^{-1} (MP4SDTQ/6–31G(dp)//MP2/6–31G(dp) + ZPVE//MP2/6–31G(dp)). The reaction proceeds exothermically through hydrogen rearrangements to yield N-protonated nitrosomethane, with an overall reaction enthalpy of –9.1 kcal mol^{-1} (MP4SDTQ/6–31G(dp)//MP2/6–31G(dp) + ZPVE//MP2/6–31G(dp)). The global minimum on the CH_4NO^+ potential hypersurface is H_2NCHOH^+, protonated formamide.

Introduction

The direct electrophilic conversions of methane to higher hydrocarbons and other derivatives are potential valuable alternatives to Fischer–Tropsch and related reactions.[2-9] Most methane functionalization methods are limited to free radical proceses (combustion, chlorination, etc.) or various stoichiometric organometallic insertion reactions.[9] Olah[10] has demonstrated that aliphatic hydrocarbons undergo substitution reactions with powerful electrophilic reagents. Strong acids promote H/D exchange; three-center two-electron (3c–2e) CHD^+ (**1**, E = D) moieties are proposed as intermediates. Similarly, alkanes can be alkylated by carbocations (via **1**, E = R). Olah has generalized such reactions within the same conceptual mechanistic framework (eq 1). Various electrophiles, E^+, also are postulated to attack a C–H bond to give 3c–2e intermediates or transition states, **1**.[10]

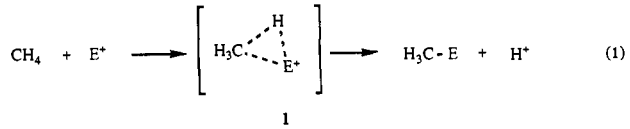

(1)

1

Although frequently proposed,[10] the mechanism of eq 1 has not been established for electrophiles other than carbocations and the proton.[11,12] We now report a model computational study involving methane and the nitrosonium ion, NO^+, as the electrophile. The results provide fundamentally new insights into the reaction mechanism which challenge the prevailing perceptions (eq 1). The gas-phase experimental[13a] and theoretical[13b] studies on aromatic substitution reactions involving NO^+ and benzene complement our investigation.

Methods

The *ab initio* Gaussian 92 program,[14a] running on an Indigo Iris XS-24 workstation, was employed to optimize geometries fully within the designated symmetry constraints at the restricted Hartree–Fock (HF)[16]

® Abstract published in *Advance ACS Abstracts*, October 1, 1993.

(1) (a) University of Georgia. (b) Universität Erlangen-Nürnberg.
(2) Muetterties, E. L.; Stein, J. *J. Chem. Rev.* **1979**, *79*, 479.
(3) Ford, P. C.; Rokocki, A. *Adv. Organomet. Chem.* **1988**, *28*, 139.
(4) Behr, A. *Angew. Chem.* **1988**, *100*, 681.
(5) Braunstein, P. *Chem. Rev.* **1988**, *88*, 681.
(6) Saillard, J. Y.; Hoffmann, R. *J. Am. Chem. Soc.* **1984**, *106*, 2006.
(7) Halpern, J. *Inorg. Chim. Acta* **1985**, *100*, 41.
(8) Crabtree, R. H. *Chem. Rev.* **1985**, *85*, 245.
(9) Ryabov, A. D. *Chem. Rev.* **1990**, *90*, 403.
(10) For reviews, see: (a) Olah, G. A.; Farooq, O.; Prakash, G. K. S. In *Activation and Functionalization of Alkanes*; Hill, C. L., Ed.; John Wiley & Sons, Inc.: New York, 1989; Chapter II, p 27 and references cited therein. (b) Olah, G. A.; Prakash, G. K. S.; Williams, R. E.; Field, L. D.; Wade, K. *Hypercarbon Chemistry*; Wiley-Interscience: New York, 1987. (c) Olah, G. A.; Prakash, G. K. S.; Summer, J. *Superacids*; Wiley-Interscience: New York, 1985.
(11) (a) Schleyer, P. v. R.; Carneiro, J. W. de M. *J. Comput. Chem.* **1992**, *13*, 997. (b) The relationship to the parent carbonium ion CH_5^+ is apparent, although, according to most recent studies (see ref 12), CH_5^+ fluctuates with essentially no barrier among C_s and C_{2v} structures. This renders all hydrogens equivalent. In this respect, CH_5^+ is unique, rather than being an appropriate model for **1**.
(12) Schreiner, P. R.; Kim, S.-J.; Schaefer, H. F.; Schleyer, P. v. R. *J. Chem. Phys.*, in press.
(13) (a) Reents W. D., Jr.; Freiser, B. S. *J. Am. Chem. Soc.* **1980**, *102*, 271. (b) Raghavachari, K.; Reents W. D., Jr.; Haddon, R. C. *J. Comput. Chem.* **1986**, *7*, 266.

0002-7863/93/1515-9659$04.00/0

level using gradient optimization techniques[15] and standard basis sets (6–31G(d), 6–31G(dp), and 6–31+G(dp)). Electron correlation was incorporated by applying second-order Møller–Plesset theory (MP2),[16,17] keeping the core electrons frozen (MP2-fc). MP4SDTQ-fc energy single-point calculations were carried out on all MP2/6–31G(dp)-optimized structures. In addition, the program PSI[14b] (running on IBM RS 6000 workstations) was used for CISD[14c]/TZ2P single-point calculations on the fully optimized MP2/6–31G(dp)//MP2/6–31G(dp) geometries for the critical structures and the transition states. The effect of unlinked quadruple excitations on the CISD energies was estimated by incorporating the Davidson correction,[14d] and the corresponding energies are denoted CISD+Q. The basis set employed for the CISD single-point calculations was the Huzinaga–Dunning triple-ζ basis set[14e]—designated for C, N, and O (10s6p/5s3p) and H (5s/3s)—with two sets of polarization functions (TZ2P) on all the nuclei. The polarization function exponents for orbitals of $l = l_v + 1$ (where l_v represents the l angular momentum value for the outermost valence shell) were $\alpha_p(H) = 1.50, 0.375$, $\alpha_d(C) = 1.50, 0.375$; $\alpha_d(N) = 1.60, 0.40$; and $\alpha_d(O) = 1.70, 0.425$. Therefore, the complete contraction scheme for the TZ2P basis set is (10s6p2d/5s3p2d) for all heavy atoms (C, N, O) and (5s2p/3s2p) for hydrogen. The d functions in the augmented basis sets were the six-component spherical harmonic functions. Analytic vibrational frequencies were obtained up to the MP2/6–31G(dp) level of theory to determine the number of imaginary frequencies (NIMAG) to characterize stationary points, where minima have NIMAG = 0 and transition structures have NIMAG = 1. Vibrational frequencies and zero-point vibrational energies (ZPVE) were scaled by the empirical factor 0.91[18] to correct for anharmonicity. All reaction enthalpies are based on MP4SDTQ/6–31G(dp) single-point energies on the optimized MP2/6–31G(dp) structures (including ZPVE at MP2/6–31G(dp)), unless stated otherwise. Standard notation[16] is used; "//" means "at the geometry of ".

Results and Discussion

Overall Substitution Process. Thermochemical Considerations. The overall reaction process is summarized in general form in eq 2:

$$\underset{\text{separated educts}}{CH_4 + E^+} \rightarrow \underset{\text{initial complex}}{CH_4\text{---}E^+} \rightarrow \underset{\substack{\text{intermediate}\\ \text{or}\\ \text{transition state}}}{[CH_4E]^+} \rightarrow \underset{\text{protonated product}}{CH_3EH^+} \xrightarrow{-H^+} \underset{\text{neutral product}}{CH_3E} \quad (2)$$

With the nitrosonium ion as the electrophile ($E^+ = NO^+$), the reaction proceeds via a weakly bound initial complex (considered below) to give the most stable N-protonated form of nitrosomethane (**6**) as the initial product (eq 3). (Other CH_4NO^+ isomers, e.g., protonated formamide (**10**), are more stable but would form subsequently. See below.) Other possible reactions, to give the H_2CNO^+ (**11**) cation and H_2 (eq 4), and hydride abstraction (eq 5)[26] are very unfavorable. In the latter case, the products would combine to give **6** (eq 6).

$$CH_4 + NO^+ \rightarrow H_3CNH{=}O^+ \ (\mathbf{6}) \qquad \Delta H_0 = -9.1 \text{ kcal mol}^{-1} \quad (3)$$

$$CH_4 + NO^+ \rightarrow H_2CNO^+ \ (\mathbf{11}) + H_2 \qquad \Delta H_0 = +28.6 \text{ kcal mol}^{-1} \quad (4)$$

$$NO^+ + CH_4 \rightarrow HNO + CH_3^+ \qquad \Delta H_0 = +74.4 \text{ kcal mol}^{-1} \quad (5)$$

$$CH_3^+ + HNO \rightarrow H_3CNH{=}O^+ \ (\mathbf{6}) \qquad \Delta H_0 = -83.5 \text{ kcal mol}^{-1} \quad (6)$$

Isoelectronic with CO, NO^+ is a well-described species, both in the gas phase[21] and as nitrosonium salts (e.g., $NO^+BF_4^-$).[10,22] The relatively high stability of NO^+ as an electrophile can be assessed by comparisons with H^+ (eq 7),[26] with CH_3^+ (eq 5),[26] and even with NO_2^+ (eq 8):[26]

$$NO^+ + H_2 \rightarrow HNO + H^+ \qquad \Delta H_0 = +167.4 \text{ kcal mol}^{-1} \quad (7)$$

$$NO^+ + HONO \rightarrow HNO + NO_2^+ \qquad \Delta H_0 = +29.8 \text{ kcal mol}^{-1} \quad (8)$$

As a consequence of the stability of NO^+, its complexation energy with CH_4 is quite low (3.6 kcal mol^{-1} at MP2/6–31+G(dp)//MP2/6–31+G(dp); see below) compared to the proton (130.0;[23] 131.6[22c] kcal mol^{-1}) and methyl cation affinities of methane (36.0;[22] 41.5[23c] kcal mol^{-1}).

Note also that the NO group stabilizes the methyl cation considerably (eq 9):

$$CH_3^+ + CH_3NO \rightarrow H_2CNO^+ \ (\mathbf{11}) + CH_4 \qquad \Delta H_0 = -54.2 \text{ kcal mol}^{-1} \quad (9)$$

(14) (a) GAUSSIAN 92, Frisch, M. J.; Trucks, G. W.; Head-Gordon, M.; Gill, P. M. W.; Wong, M. W.; Foresman, J. B.; Johnson, B. G.; Schlegel, H. B.; Robb, M. A.; Replogle, E. S.; Gomperts, R.; Andres, J. L.; Raghavachari, K.; Binkley, J. S.; Gonzales, G.; Martin, R. L.; Fox, D. J.; DeFrees, D. J.; Baker, J.; Stewart, J. J. P.; Pople, J. A., Eds.; Gaussian, Inc.: Pittsburgh, PA, 1992. (b) PSITECH Inc., Watkinsville, GA. (c) Brooks, B. R.; Laidig, W. D.; Saxe, P.; Goddard, J. D.; Yamaguchi, Y.; Schaefer, H. F. *J. Chem. Phys.* **1980**, *72*, 4625. Rice, J. E.; Amos, R. D.; Handy, N. C.; Lee, T.; Schaefer, H. F. *J. Chem. Phys.* **1986**, *85*, 963. (d) Langhoff, S. R.; Davidson, E. R. *Int. J. Quantum. Chem.* **1974**, *8*, 61. (e) Dunning, T. H., Jr. *J. Chem. Phys.* **1971**, *55*, 716.

(15) Broyden, C. G. *J. Math. Appl.* **1970**, *6*, 222. Fletcher, R. *Comput. J.* **1970**, *13*, 370. Goldfarb, D. *Math. Comput.* **1970**, *24*, 647. Shanno, D. F. *J. Optim. Theory Appl.* **1985**, *46*, 87.

(16) Hehre, W. J.; Radom, L.; Pople, J. A.; Schleyer, P. v. R. *Ab Initio Molecular Orbital Theory*; John Wiley & Sons, Inc.; New York, 1986.

(17) Møller, C.; Plesset, M. S.; *Phys. Rev.* **1934**, *46*, 618. Binkley, J. S.; Pople, J. A. *Int. J. Quantum Chem.* **1975**, *9*, 229. Pople, J. A.; Binkley, J. S.; Seeger, R. *Int. J. Quantum Chem.* **1976**, *S10*, 1.

(18) Grev, R. S.; Janssen, C.; Schaefer, H. F. *J. Chem. Phys.* **1991**, *95*, 5128.

(19) Feller, D. *J. Chem. Phys.* **1992**, *96*, 6104.

(20) Reed, A. E.; Curtiss, L. A.; Weinhold, F. *Chem. Rev.* **1988**, *88*, 899.

(21) (a) Huber, K. P.; Herzberg, G. *Constants of Diatomic Molecules*; Van Nostrand Reinhold: New York, 1979, p 482. (b) JANAF Thermochemical Tables. Chase, M. W., Jr.; Davies, C. A.; Downey J. R., Jr.; Frurip, D. J.; McDonald, R. A.; Syverud, A. N. *J. Phys. Chem. Ref. Data* **1985**, *14*, Suppl. 1, 1534. (c) Lias, S. G.; Bartmess, J. E.; Liebmann, J. F.; Holmes, J. L.; Levin, R. D.; Mallard, W. G. *J. Phys. Chem. Ref. Data* **1988**, *17*, Suppl. 1, 1.

(22) For application of nitrosonium salts, see: (a) Olah, G. A. Methods for Preparing Energetic Nitrocompounds: Nitration with Superacid Systems, Nitronium Salts, and Related Complexes. *Chemistry of Energetic Materials*; Academic Press: New York, 1991; p 139. (b) Prakash, G. K. S.; Wang, Q.; Li, X. Y.; Olah, G. A. *New J. Chem.* **1990**, *14*, 791. (c) Olah, G. A.; Herges, R.; Felberg, J. D.; Prakash, G. K. S. *J. Am. Chem. Soc.* **1985**, *107*, 5282. (d) Olah, G. A.; Arvanaghi, M.; Ohannesian, L.; Prakash, G. K. S. *Synthesis* **1984**, *9*, 785. (e) Olah, G. A.; Ho, T. L. *Synthesis* **1976**, *9*, 610.

(23) Carneiro, J. W. de M.; Schleyer, P. v. R.; Saunders, M.; Remington, R.; Schaefer, H. F.; Arvi, R.; Sorensen, T. S. *J. Am. Chem. Soc.*, submitted for publication.

(24) Pepper, M.; Schavitt, I.; Schleyer, P. v. R.; Janoschek, R.; Quack, M. *J. Am. Chem. Soc.*, submitted for publication.

(25) Schleyer, P. v. R.; Tidor, B.; Jemmis, E. D.; Chandrasekhar, J.; Würthwein, E.-U.; Kos, A. J.; Luke, B. T.; Pople, J. A. *J. Am. Chem. Soc.* **1983**, *105*, 484.

(26) The experimental values (see refs 21b,c), based upon heats of formation at 0 K, for these thermochemical equations (eq 5, $\Delta H_f^\circ = 67.8$ kcal mol^{-1}; eq 7, $\Delta H_f^\circ = 154.4$ kcal mol^{-1}; eq 8, $\Delta H_f^\circ = 39.7$ kcal mol^{-1}) do not agree well with our computed results, due to the difficulty in describing the *free* species NO^+ accurately. In fact, only the coupled cluster method (CCSD), in conjunction with a TZ2P basis set, reproduces the experimental bond lenght (1.063 Å, see ref 21a, CCSD TZ2P = 1.060 Å). Other methods ar larger in error: HF/6–31G(d) = 1.040 Å; MP2/6–31G(d) = 1.103 Å; MP2/6–31G(3df) = 1.080 Å; CISD TZ2P = 1.052 Å).

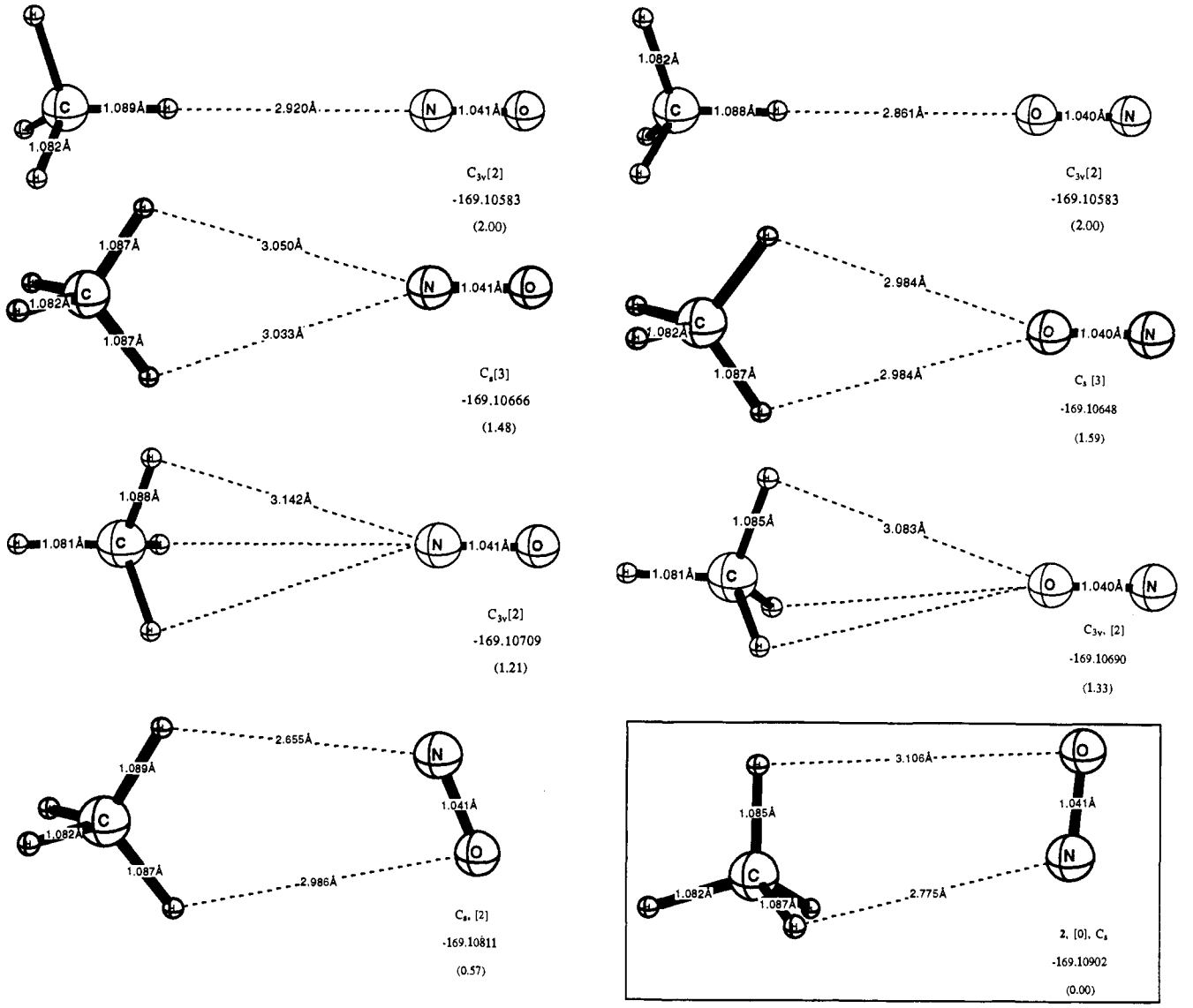

Figure 1. Eight possible complexes of $CH_4 + NO^+$; geometric parameters, absolute energies (in au) and relative energies versus **2** (in parentheses in kcal mol^{-1}) at the HF/6-31G(d) level of theory. The number of imaginary vibrational frequencies, given in brackets, shows that only **2** is a minimum.

Table I. Relative (in kcal mol^{-1}) and Absolute (in au) Energies for the Reaction CH_4- - -NO^+ Complex (**2**) → TS_{23} → H_4C–NO^+ (**3**) at Various Levels of Theory[a]

	HF/ 6-31G(d)	HF/ 6-31G(dp)	MP2/6-31G(d)// MP2/6-31G(d)	MP2/6-31G(dp)// MP2/6-31G(dp)	MP4/6-31G(dp)// MP2/6-31G(dp)	CISD/TZ2P// MP2/6-31G(dp)	CISD+Q/TZ2P// MP2/6-31G(dp)
2	169.109 02	169.115 78	169.581 74	169.614 02	169.656 42	169.671 77	169.735 99
E_{rel}	0.0	0.0	0.0	0.0	0.0	0.0	0.0
ZPVE	34.8	31.4	32.7	30.0	30.0[b]	30.0[b]	30.0[b]
E_{rel} + ZPVE	0.0	0.0	0.0	0.0	0.0	0.0	0.0
TS_{23}	168.989 96	169.005 09	169.470 20	169.505 31	169.548 27	169.574 77	169.640 30
E_{rel}	74.7	69.5	70.0	68.2	67.9	60.9	60.0
ZPVE	29.7	29.6	27.7	27.6	27.6[b]	27.6[b]	27.6[b]
E_{rel} + ZPVE	69.1	67.4	65.0	65.7	65.5	58.5	57.6
3	168.995 52	169.010 74	169.471 17	169.505 69	169.549 37	169.576 06	169.641 04
E_{rel}	71.2	65.9	69.4	67.8	67.2	60.0	59.6
ZPVE	30.5	30.5	27.9	27.7	27.7[b]	27.7[b]	27.7[b]
E_{rel} + ZPVE	66.5	65.0	64.1	65.5	64.9	57.7	57.3

[a] Zero-point vibrational energy corrections (ZPVE, scaled by 0.91) in kcal mol^{-1}, MP2 and MP4 in frozen core approximation. [b] ZPVE at MP2/6-31G(dp).

CH4---NO$^+$ Complex. A weakly bound complex of methane with the nitrosonium ion is formed first:

$$CH_4 + NO^+ \rightarrow \underset{2}{H_4C{-}{-}{-}NO^+} \qquad (10)$$

The most favorable structure of this H_4C---NO^+ complex, **2**, has NO^+ bound side-on to CH_4; seven other possibilities are depicted in Figure 1, along with their relative energies versus **2**.

The exothermicity of eq 10 increases significantly from the Hartree–Fock level (HF/6-31G(dp)//HF/6-31+G(dp) + ZPVE//HF/6-31+G(dp): −2.2 kcal mol^{-1}) to the correlated level (MP4SDTQ/6-31+G(dp)//MP2/6-31+G(dp) + ZPVE//MP2/6-31+G(dp): −3.7 kcal mol^{-1}). The inclusion of diffuse functions should largely overcome[19] basis set superposition

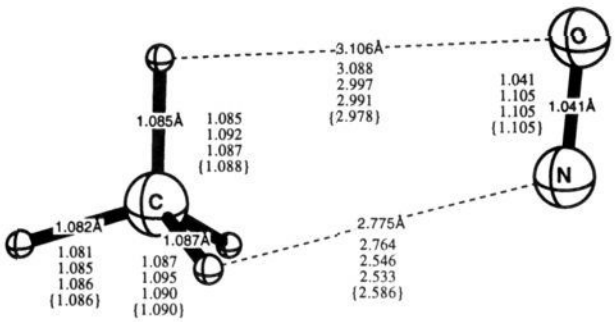

2 , C_s

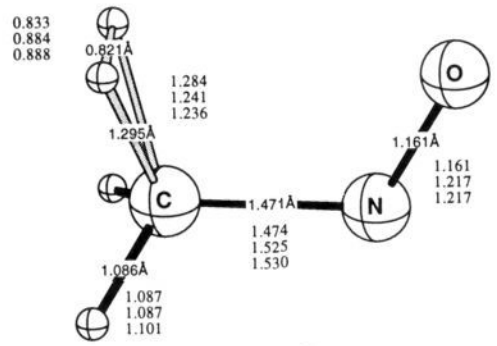

3 , C_s

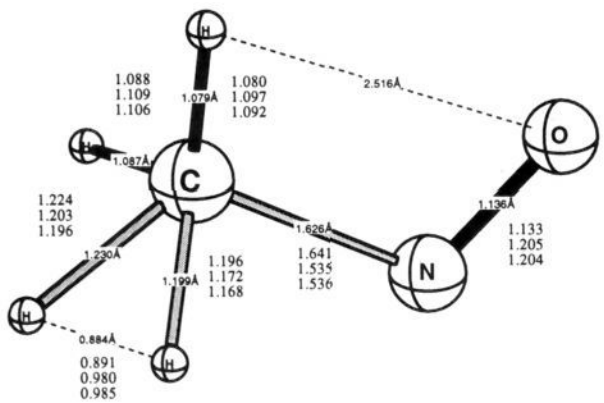

TS_{23} , C_1

1. HF/6-31G(d) (in bonds)
2. HF/6-31G(dp)
3. MP2/6-31G(d)//MP2/6-31G(d)
4. MP2/6-31G(dp)//MP2/6-31G(dp)

Figure 2. Geometrical parameters of the three critical structures, **2** (C_s), TS_{23} (C_1), and **3** (C_s), in the reaction of methane with NO^+ at different levels of theory. For **2**, the MP2/6–31+G(dp)-optimized structure is given in curly brackets, { }. At this level, the bond lengths for the isolated species are NO^+ (1.103 Å) and CH_4 (1.086 Å).

errors (BSSE). The increasing stability of the complex (from SCF to MP2) is reflected in a lengthening of the N–O and C–H bonds as well as a shortening of the N- - -H bond distances (Figure 2).

The binding in **2** is mainly due to the polarization of methane by NO^+, although some covalent contributions (accounting for 1.3 kcal mol^{-1}, natural population analysis[20] at MP2/6–31+G(dp)//MP2/6–31+G(dp), Figure 3) arise from two of the σ (CH) orbitals donating in the appropriate π^* (NO^+) orbital and the nitrogen lone pair donating into an antibonding σ^* (CH) orbital.

The Reaction Step CH4—NO^+ → TS → H_4C—NO^+. In the current mechanistic model, depicted in eq 1,[10] a C–H bond is attacked by the electrophile. This is certainly very reasonable

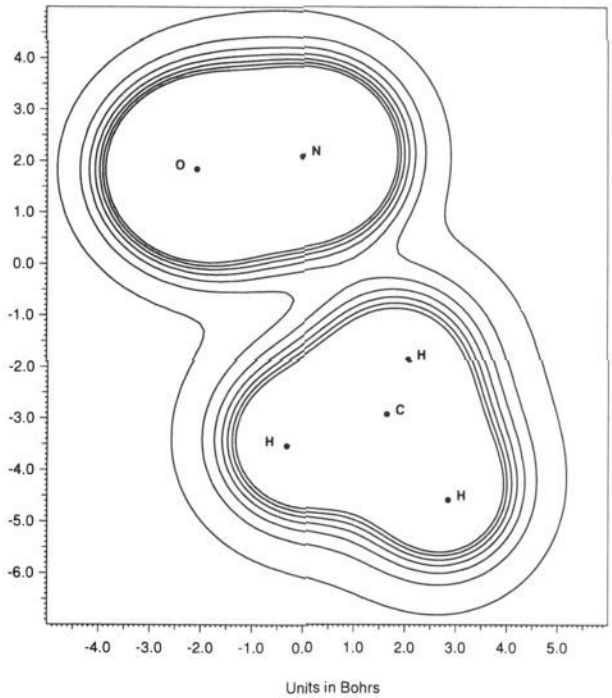

Figure 3. Total electron density plot of the complex (**2**, C_s) of CH_4 and NO^+. Note, however, that electrostatic polarization is the main contributor to the binding.

for H^+ since an essentially symmetrical 3c–2e CH_2^+ bonding arrangement can result. However, most electrophiles are more stable than H^+ and are *unlikely* to engage in such 3c–2e CHE^+ bonding since the necessary balance is lacking.

The attack of the nitrosonium ion on the carbon of methane proceeds via the transition state TS_{23}, which has no symmetry (C_1 point group), to give the C_s intermediate **3** (which is described in detail below). Relative[27] and absolute energies for **2**, **3**, and TS_{23} are given in Table I.

Increase in computational sophistication decreases the energy difference between TS_{23} and structure **3**; this becomes only 0.3 kcal mol^{-1} at our highest level of theory. Nevertheless, the structures of TS_{23} and **3** are different, although both have 3c–2e CHH^+ moieties. The optimization of TS_{23} at the correlated levels of theory was very difficult. The potential energy hypersurface is flat in the direction of **3**, but steep toward **2**. The harmonic vibrational frequencies show the same trend: the low frequencies for TS_{23} increase with a larger basis set at the correlated level, while the lowest frequencies for **3** decrease (frequencies available as supplementary material). We also were unable to find a transition structure leading from **3** to the next intermediate (**4**), as this process appears to have a very low barrier. The two hydrogens involved in the 3c–2e of structure **3** usually couple as the depicted transition states demonstrate. Following just a particular C–H mode is therefore not a straightforward optimization. Hence, we conclude that **3** is not a very stable local minimum.

Our results suggest that electrophiles can be regarded as attacking carbon, rather than the electrons constituting a C–H bond. How can this unusual mode of reaction be understood? Tetrahedral methane has no lone pairs, and there is no obvious reason for an electrophile to attack carbon. Distorted forms of methane, e.g., in planar (D_{4h} or C_{2v}), pyramidal (C_{4v}), or C_s symmetry (**3a**, X = lone pair), do have lone pairs which may bind

(27) The large activation energy is not surprising. The reaction of the isoelectronic CO with methane to give H_3CCHO would have an even higher barrier. Stronger electrophiles than NO^+ have a considerably lower barrier, as we will show in a subsequent publication.

Figure 4. Schematic MO description of the bonding in **3**, which may be qualitatively described as methylene binding to NO^+ and H_2.

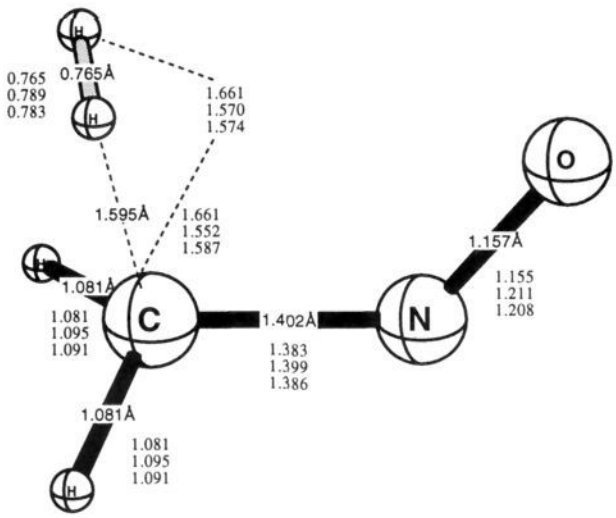

Figure 5. The geometrical parameters of the transition structure (TS_{loss}, C_1) for the loss of H_2 from H_4C–NO^+ (**3**), leading to the stable H_2C–NO^+ cation and H_2.

an electrophile, but these arrangements are much higher in energy.

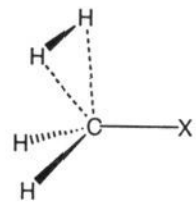

3a

The C_s form of methane[24] (**3a**, with X representing a lone pair) can be regarded as a complex between singlet methylene and H_2 and is closely structurally related to **3**. Even though the distortion energy of methane to **3a** (X = lone pair; eq 11) is very large, attachment of the electrophile would provide partial compensation. This is well illustrated with an ionic electrophile, Li^+. The binding energy of Li^+ to a "face" of T_d methane is only moderate (eq 12) but to C_s CH_4 is 43.9 kcal mol^{-1} larger (to give **3a**, where X = Li^+; eq 13). As a consequence of this difference, the distortion energy of the Li^+---CH_4 complex (eq 14) is much less than that of methane itself (eq 11). *Of course, the distortion of methane would not proceed as a separate step, but would occur simultaneously with the attack of an electrophile (e.g., to give 3 or 3a, where X = E$^+$).*

Intermediate **3** also can be regarded as a complex between the stabilized H_2CNO^+ cation (see eq 9) and H_2. This arrangement is much more likely than a highly unsymmetrical alternative with a three-center two-electron bond between C, H, and NO^+ (**1**, E^+ = NO^+). The structure of **3** can also be visualized as singlet methylene bound to the electrophile NO^+ via its lone pair and to molecular hydrogen via the empty p orbital (Figure 4). The energies of formation of **3** (eq 15) and of **3a** (X ≈ Li^+, a $LiCH_2^+$ cation complexed to H_2 (eq 16)) compare nicely. This situation

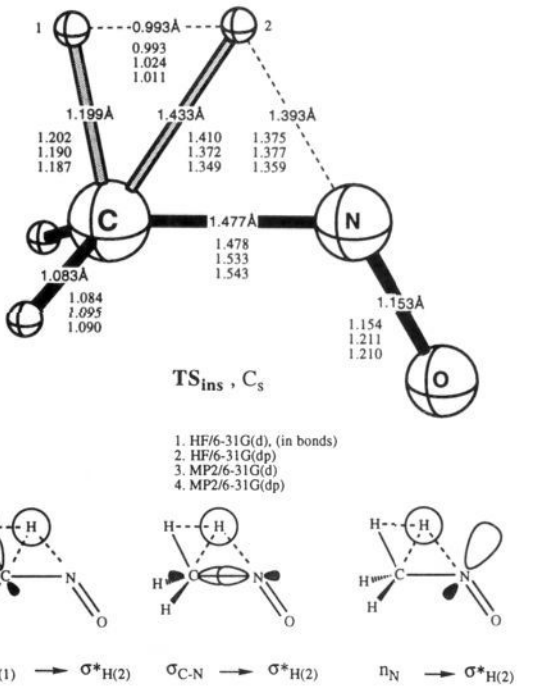

Figure 6. The geometry of the transition state (TS_{ins}, C_s) for the insertion of NO^+ into a C–H bond of methane. Three of the binding molecular orbitals also are depicted schematically; the labels describe the types of interaction.

$$CH_4\ (T_d) \rightarrow CH_4\ (C_s, \mathbf{3a}, X = \text{lone pair}) \qquad \Delta H_0 = +118.9\ \text{kcal mol}^{-1} \quad (11)$$

$$CH_4\ (T_d) + Li^+ \rightarrow HCH_3\text{---}Li^+\ (C_{3v}) \qquad \Delta H_0 = -10.9\ \text{kcal mol}^{-1} \quad (12)$$

$$CH_4\ (C_s) + Li^+ \rightarrow H_4C\text{–}Li^+\ (C_s, \mathbf{3a}, X = Li^+) \qquad \Delta H_0 = -54.8\ \text{kcal mol}^{-1} \quad (13)$$

$$HCH_3\text{---}Li^+\ (C_{3v}) \rightarrow H_4C\text{–}Li^+\ (C_s, \mathbf{3a}, X = Li^+) \qquad \Delta H_0 = +74.9\ \text{kcal mol}^{-1} \quad (14)$$

$$CH_4\ (T_d) + NO^+ \rightarrow H_4C\text{–}NO^+\ (C_s) \qquad \Delta H_0 = 61.3\ \text{kcal mol}^{-1} \quad (15)$$

$$CH_4\ (T_d) + Li^+ \rightarrow H_4C\text{–}Li^+\ (C_s, \mathbf{3a}, X = Li^+) \qquad \Delta H_0 = 64.1\ \text{kcal mol}^{-1} \quad (16)$$

will change for electrophilic substitution reactions of branched hydrocarbons, where more stable carbenium ions can form. We will report such examples subsequently.

Note that **3** and CH_5^+ are very different. Loss of hydrogen from CH_5^+ is highly endothermic (eq 17), whereas loss of H_2 from **3** is exothermic (eq 18). Nevertheless, the latter reaction does *not* occur spontaneously, as a significant activation barrier (involving TS_{loss}, Figure 5) of 2.8 kcal mol^{-1} (MP4STDQ/6–

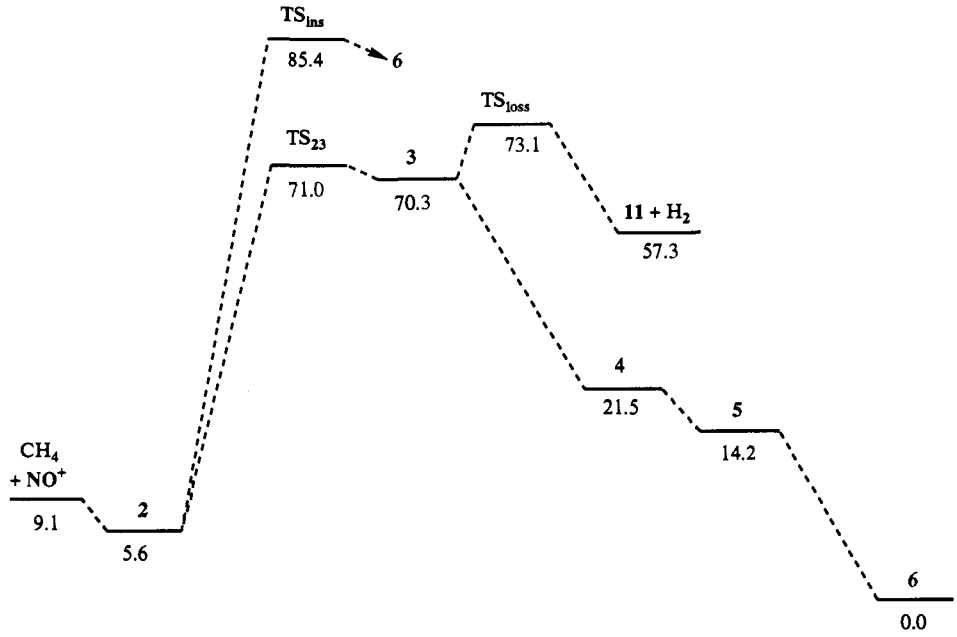

Figure 7. The reaction path of $CH_4 + NO^+$: relative energies at MP4SDTQ/6–31G(dp)//MP2/6–31G(dp) + ZPVE//MP2/6–31G(dp) in kcal mol^{-1}. Structure **6** is the zero of energy for this diagram.

31G(dp)//MP2/6–31G(dp) + ZPVE//MP2/6–31G(dp)) must be overcome. In contrast, there is no barrier for the attachment of H_2 to CH_3^+ (the reverse reaction of eq 17).

$$CH_5^+ \rightarrow CH_3^+ + H_2 \qquad \Delta H_0 \text{ (expt}^{21c}\text{)} = 45.3 \text{ kcal mol}^{-1}$$

$$\Delta H_0 \text{ (theor}^{11a}\text{)} = 42.0 \text{ kcal mol}^{-1} \quad (17)$$

$$\mathbf{3} \rightarrow H_2CNO^+ \text{ (11)} + H_2 \qquad \Delta H_0 = -32.6 \text{ kcal mol}^{-1} \quad (18)$$

A possible H_2 dissociation–association mechanism (through eq 18) to, for example, the possible product $H_2C{=}NHOH^+$ (**8**, C_1) is exothermic by −88.5 kcal mol^{-1} (ΔH_0 for the hypothetic reaction of **3** to **8**). However, the reaction more likely proceeds via hydrogen rearrangements since **4** is 35.8 kcal mol^{-1} lower in energy than **11** + H_2 (cf. Figure 7).

Addition versus Insertion into a C–H Bond. We also investigated the insertion process of NO^+ into a C–H bond. At the MP4SDTQ/6–31G(dp)//MP2/6–31G(dp) + ZPVE//MP2/6–31G(dp) level, the transition state (TS_{ins}) for this reaction mode is 14.4 kcal mol^{-1} higher in energy than the transition state for the addition process (TS_{23}). The insertion transition structure (TS_{ins}), depicted in Figure 6, does not involve 3c–2e bonding and is best described in terms of multicenter bonding (H(1), H(2), C, and N), using more than one molecular orbital (see Figure 6 for depictions of three of the binding molecular orbitals). The interatomic distances make this point very clear: one can recognize an H_2 subunit comprising H(1) and H(2), more distant from carbon than the other two, tightly bound hydrogens. The central hydrogen, H(2), is farthest from carbon and bridges between nitrogen and H(1).

Moreover, the rather large energy difference of 14.4 kcal mol^{-1} between the two transition states (TS_{23} and TS_{ins}) suggests that there is no equilibrium between different types of 3c–2e structures **13** and **14** (eq 19). Although the thermodynamically most stable final product, **6**, can be reached through TS_{ins}, the larger activation barrier makes this reaction mode unlikely.

Thus, the situation for **3**, the H_2---CH_2NO^+ intermediate, is quite different from CH_5^+, where complete hydrogen scrambling

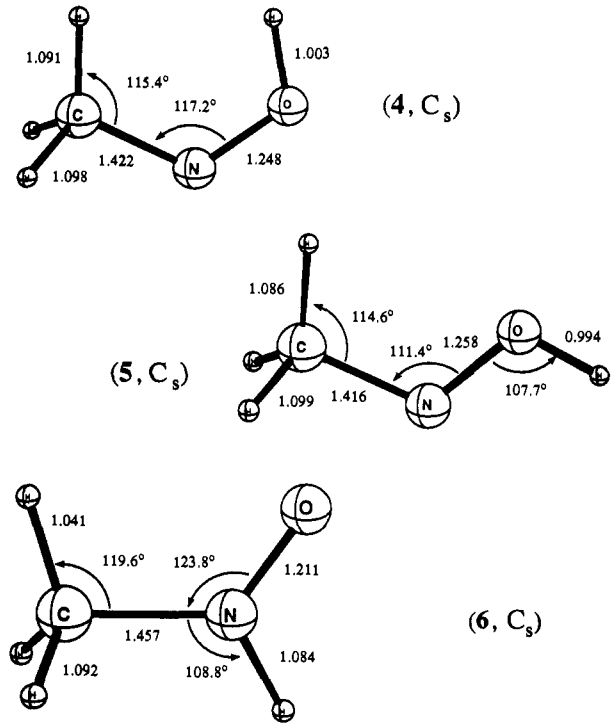

Figure 8. Products derived from the hydrogen rearrangements in the reaction **4** → **6**; geometric parameters given at the MP2/6–31G(dp)//MP2/6–31G(dp) level of theory.

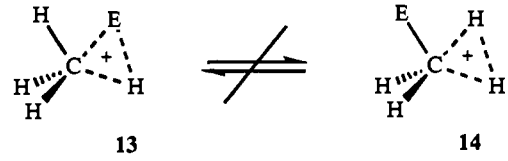

13 **14** (19)

(where E is neither H nor C)

occurs essentially without any barrier.[11,12] In contrast, we found no indication of CEH^+ 3c–2e bonding (**13**). The nonequivalence of the C–E, C–H, and H–H binding energies renders such arrangements unlikely, since the necessary balance will not be achieved.

Table II. Absolute Energies (in –au) of the CH_4NO^+ Structures at Various Levels of Theory

	HF/6-31G(d)	HF/6-31G(dp)	MP2/6-31G(d)// MP2/6-31G(d)	MP2/6-31G(dp)// MP2/6-31G(dp)	MP2/6+31G(dp)// MP2/6+31G(dp)	MP4[a]/6-31G(dp)// MP2/6-31G(dp)
$CH_4 + NO^+$	169.104 82	169.111 35	169.575 14	169.606 95	169.655 80	169.649 55
2	169.109 02	169.115 78	169.581 84	169.614 02	169.619 81	169.656 42
TS_{23}	168.989 96	169.005 09	169.470 20	169.505 31		169.548 27
TS_{ins}	168.959 40	168.977 47	169.443 62	169.481 68		169.524 37
3	168.995 52	169.010 74	169.471 17	169.505 96		169.548 27
TS_{loss}	168.992 60	169.004 34	169.463 21	169.495 45		169.541 77
4	169.098 89	169.110 81	169.557 20	169.588 22		169.635 33
5	169.112 18	169.123 92	169.568 32	169.600 66		169.647 30
6	169.131 91	169.140 82	169.598 94	169.629 58		169.670 58
7	169.092 86	169.107 01	169.555 96	169.590 41		169.632 97
8	169.169 93	169.184 31	169.625 76	169.660 08		169.701 22
9	169.139 99	169.151 06	169.604 87	169.636 57		169.675 48
10	169.266 55	169.283 75	169.721 04	169.757 20		169.794 48
11 + H_2	169.035 72	169.044 31	169.520 82	169.548 49		169.594 87
12	169.261 73	169.278 83	169.918 16	169.751 88		169.789 29

[a] MP4SDTQ-fc.

Further Rearrangements to More Stable Isomers. The reaction (Figure 7) can proceed exothermically from **3** to **6** by simple hydrogen rearrangements (Figures 7 and 8; Tables II and III) via **4** (C_s, O-protonated *syn*-nitrosomethane) and **5** (C_s, O-protonated *anti*-nitrosomethane).

While N-protonated nitrosomethane (**6**, C_s) is the likely product, we also located additional CH_4NO^+ minima **7** (C_1, O-protonated oxaziridine), **8** (C_1, N-protonated hydroxylamine), **9** (C_1, N-protonated oxaziridine), and **12** (C_s, O-protonated *anti*-formamide) as well as the global minimum **10** (C_s, O-protonated *syn*-formamide) (Figure 9; Tables IV and V, supplementary material). All of these structures are not necessarily related to the process described in this paper—even though **8** and **9** and especially **10** and **12** have much lower energies than **6**—since the rearrangement from **6** to **7** is endothermic by 24.7 kcal mol^{-1} and presumably involves a considerable activation barrier, as the reaction would require a forbidden [1,3] hydrogen shift. The same argument is valid for the reaction of **6** to **8**, omitting **7**. At some point, an unfavorable cyclic structure must be involved to eventually reach the global minimum **10**. Although those reactions are exothermic overall, the barriers are expected to be high because the strong N–O bond must be broken in the critical step.

Conclusions

The nitrosonium cation attacks methane electrophilically at carbon rather than at a C–H bond. The preferred transition structure (TS_{23}) exhibits three-center CHH^+ bonding and is only slightly higher in energy than the intermediate **3**. This species also utilizes 3c–2e CHH^+ bonding on an H_2 unit attached to the H_2CNO^+ cation. There is no evidence that 3c–2e CHE^+ species (**1**, **13**) are involved. An alternative transition structure for C–H attack (TS_{ins}) is 14.4 kcal mol^{-1} higher in energy than TS_{23}, and its multicenter bonding is more complex. The abstraction of a hydride ion from methane by NO^+ (eq 5) also is unfavorable. This unexpected mode of NO^+ attack at the carbon of methane can be visualized as involving methane distortion which enables carbon to bind the electrophile to the developing lone pair. Part of the energy required for the distortion is recovered from the new bonding interaction, as these can occur simultaneously. The activation energy, 57.6 kcal mol^{-1} at CISD+Q/TZ2P//MP2/6-31G(dp) + ZPVE//MP2/6-31G(dp), is quite large, but this is due to the exceptional stability of NO^+.[27] The reaction proceeds exothermically from **3** through hydrogen rearrangements to yield N-protonated nitrosomethane (**6**) with an overall reaction enthalpy (vs NO^+ and CH_4) of –9.1 kcal mol^{-1} (MP4SDTQ/6-31G(dp)//MP2/6-31G(dp) + ZPVE//MP2/6-31G(dp)). Additional CH_4NO^+ minima were found (**7**–**10**, **12**). Protonated formamide (**10**) is the global minimum.

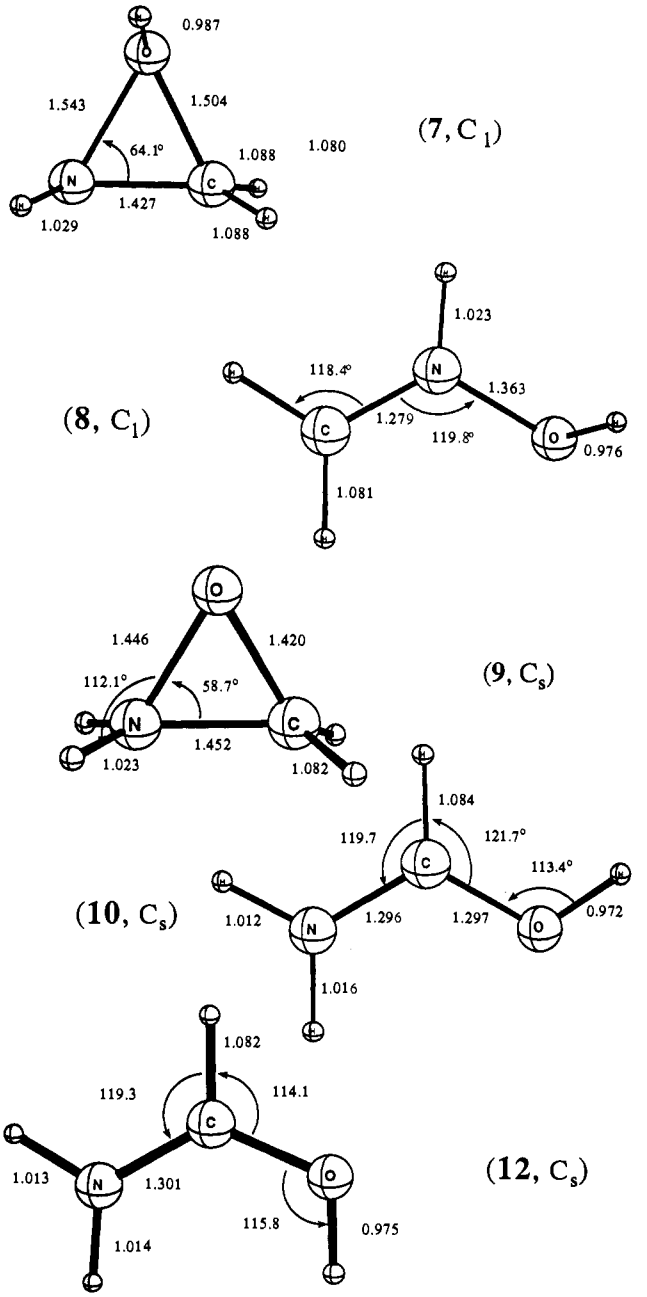

Figure 9. Further minima of CH_4NO^+. All geometrical parameters were optimized at the MP2/6–31G(dp) level. These structures are lower in energy than **6** but can only be reached through an endothermic pathway via **6**. The global minimum is protonated formamide, **10**.

Table III. Relative Energies of the CH_4NO^+ Structures versus **10** at Various Levels of Theory (in kcal mol^{-1}), Including ZPVE Corrections at the Indicated Levels of Theory

	HF/6-31G(d)	HF/6-31G(dp)	MP2/6-31G(d)// MP2/6-31G(d)	MP2/6-31G(dp)// MP2/6-31G(dp)	MP4[a,b]/6-31G(dp)// MP2/6-31G(dp)
$CH_4 + NO^+$ [a]	43.5	13.6	11.0	10.2	9.1
2	10.0	8.4	4.6	3.5	5.6
TS_{23}	79.8	76.0	73.0	69.3	70.8
TS_{ins}	101.4	96.3	91.1	86.6	86.0
3	77.2	73.4	72.0	69.0	70.3
TS_{loss}	79.6	79.9	77.6	76.5	73.1
4	19.0	17.4	25.6	25.4	21.5
5	11.4	9.9	18.9	17.8	14.2
6	0.0	0.0	0.0	0.0	0.0
7	25.3	22.2	28.1	25.7	24.7
8	−23.2	−26.5	−16.1	−18.3	−18.1
9	−3.2	−4.5	−1.6	−2.4	−0.9
10	−83.0	−87.9	−74.7	−78.0	−75.7
11 + H_2	48.0	49.9	39.5	10.9	57.3
12	−80.0	−84.8	−72.9	−74.7	−72.4

[a] MP4SDTQ-fc. [b] Including ZPVE at MP2/6-31G(dp).

Acknowledgment. The authors thank Prof. G. A. Olah for lively and very fruitful discussions. The work in Erlangen was supported by the Deutsche Forschungsgemeinschaft, the Fonds der Deutschen Chemischen Industrie (fellowship for P.R.S.), and the Convex Computer Corporation. The work in Georgia was supported by the U.S. Department of Energy, Office of Basic Energy Sciences, Division of Chemical Sciences, Fundamental Interactions Branch, Grant DE-FG09-87ER13811. P.R.S. thanks Prof. R. K. Hill for helpful comments, and J. R. "Quatsch" Thomas for help with literature searching.

Supplementary Material Available: Vibrational frequencies at the MP2(fc)/6–31G(dp) level for structures **2**, TS_{23}, and **3** (3 pages). Ordering information is given on any current masthead page.